Proton Relay in a One-Dimensional Hydrogen-Bonded Chain Composed of Water Molecules and a Squaric Acid Derivative

Hiroshi Terao,[†] Tadashi Sugawara,*[,†] Yasuo Kita,[‡] Naoki Sato,[‡] Eriko Kaho,[§] and Sadamu Takeda[§]

Contribution from the Department of Basic Science, Graduate School of Arts and Sciences, The University of Tokyo, Meguro, Tokyo 153-8902, Japan, Institute for Chemical Research, Kyoto University, Uji, Kyoto 611-0011, Japan, and Division of Chemistry, Graduate School of Science, Hokkaido University, Sapporo 060-0810, Japan

Received February 26, 2001. Revised Manuscript Received June 26, 2001

Abstract: The crystal structure of a hydrated crystal of bis(squaryl)biphenyl (**BSQB**·$4H_2O$), in which two squaric acid moieties are connected with a 4,4′-biphenyl unit, was characterized by the presence of a one-dimensional hydrogen-bonded chain composed of **BSQB** and water molecules. X-ray crystallographic analysis showed that **BSQB** exists in a dianion form and that, on average, two of the four water molecules are protonated. The enhanced temperature dependence of the thermal parameters of the oxygen atoms of the water molecules suggested dynamic disorder of the water molecules. The solid-state magic angle spinning deuterium NMR spectrum of **BSQB**·$4D_2O$ revealed that deuterons are exchanged between heavy water molecules and oxonium ions with an exchange rate of ca. 700 Hz around 250 K and that deuterons start to migrate in a hydrogen-bonded cluster of water molecules. Ac dielectric measurements were also used to examine the dynamic process in the hydrated crystal. The dielectric permittivity of the crystal dramatically increased above 250 K with a distinct frequency dependence ($\epsilon' = 4.7 \times 10^4$ at 340 K and 1 kHz). The frequency dependence of tan δ at 290 K exhibited a maximum at 3.0 kHz, and this maximum shifted to lower frequencies when the temperature of the crystal decreased. These experimental results suggested that in the one-dimensional hydrogen-bonded chain of **BSQB**·$4H_2O$ a proton relay between oxonium ions and water molecules occurred within a cluster of four water molecules and that the relay was transmitted to the adjacent cluster mediated by the modulation of the negative charge distribution of the **BSQB** dianion. These phenomena were interpreted as the solitonic migration of the charged domain boundaries along the one-dimensional hydrogen-bonded chain.

Introduction

Proton transfer along a one-dimensional (1D) hydrogen-bonded chain of water molecules has drawn much attention not only from the theoretical aspect of solitonic charge transport[1] but also from the viewpoint of biological functions such as active proton transport in membrane proteins, e.g., cytochrome oxidase[2] and bacteriorhodopsin.[3] A recent high-resolution X-ray crystallographic analysis[4] revealed that a number of water pools exist between the amino acid residues of cytochrome *c* oxidase; these clusters of water molecules play a crucial role in active proton transport. To understand the intrinsic nature of proton transport, it is important to carry out model studies, but no such investigations have been reported because of the difficulty of constructing a 1D hydrogen-bonded chain composed of water molecules.

Along these lines, we are interested in a 1D hybrid hydrogen-bonded chain composed of water molecules and a highly acidic β-hydroxyenone, which can transport a proton from its hydroxyl group to a carbonyl group of the adjacent molecule. Squaric acid, which has two orthogonally located β-hydroxyenones, is the sole example of a hydrogen-bonded crystal, which exhibits intermolecular proton-transfer coupled with a polarity inversion of the π-conjugated electronic system, even though the crystal does not contain any water molecules. The crystal exhibits a pronounced dielectric response above 371 K as revealed by correlated polarity inversion.[5] Expecting to observe a cooperative intermolecular proton transfer in 1D hydrogen-bonded β-hydroxyenones involving water molecules, we synthesized a new squaric acid derivative, bis(squaryl)biphenyl (**BSQB**), in which two squaryl groups are separated by the 4,4′-biphenyl unit. For **BSQB** to exhibit a 1D character in a hydrogen-bonded system, the electronic coupling between the two squaryl groups in **BSQB**

* To whom correspondence should be addressed.
[†] The University of Tokyo.
[‡] Kyoto University.
[§] Hokkaido University.

(1) (a) Zolotaryuk, A. V.; Pnevmatikos, St.; Savin, A. V. *Phys. Rev. Lett.* **1991**, *67*, 707−710. (b) Howard, I. A.; Sharma, R.; Mittal, R. *Physica D* **1998**, *133*, 212−217. (c) Antonchenko, V. Ya.; Davydov, A. D.; Zolotariuk, A. V. *Phys. Status Solidi B* **1983**, *115*, 631−640. (d) Kashimori, Y.; Kikuchi, T.; Nishimoto, K. *J. Chem. Phys.* **1982**, *77*, 1904−1907. (e) Pnevmatikos, S. *Phys. Rev. Lett.* **1988**, *60*, 1534−1537.

(2) Yoshikawa, S.; Shinzawa-Itoh, K.; Nakashima, R.; Yaono, R.; Yamashita, E.; Inoue, N.; Yao, M.; Fei, M. J.; Libeu, C. P.; Mizushima, T.; Yamaguchi, H.; Tomizaki, T.; Tsukihara, T. *Science* **1998**, *280*, 1723−1729.

(3) (a) Luecke, H.; Schobert, B.; Richter, H. T.; Cartailler, J. P.; Lanyi, J. K. *Science* **1999**, *286*, 255−261. (b) Gennis, R. B.; Ebrey, T. G. *Science* **1999**, *286*, 252−253. (c) Henderson, R.; Baldwin, J. M.; Ceska, T. A.; Zemlin, F.; Beckmann, E.; Downing, K. H. *J. Mol. Biol.* **1990**, *213*, 899−929. (d) Nagle, J. F.; Tristram-Nagle, S. *J. Membr. Biol.* **1983**, *74*, 1−14. (e) Edman, K.; Nollert, P.; Royant, A.; Belrhali, H.; Pebay-Peyroula, E.; Hajdu, J.; Neutze, R.; Landau, E. M. *Nature* **1999**, *401*, 822−826.

(4) Tsukihara, T.; Aoyama, H.; Yamashita, E.; Tomizaki, T.; Yamaguchi, H.; Shinzawa-Itoh, K.; Nakashima, R.; Yaono, R.; Yoshikawa, S. *Science* **1996**, *272*, 1136−1144.

(5) (a) Semmingsen, D.; Hollander, F. J.; Ketzle, T. F. *J. Chem. Phys.* **1979**, *66*, 4405−4412. (b) Samara, G. A.; Semmingsen, D. *J. Chem. Phys.* **1979**, *71*, 1401−1407.

10.1021/ja010519a CCC: $20.00 © 2001 American Chemical Society
Published on Web 10/05/2001

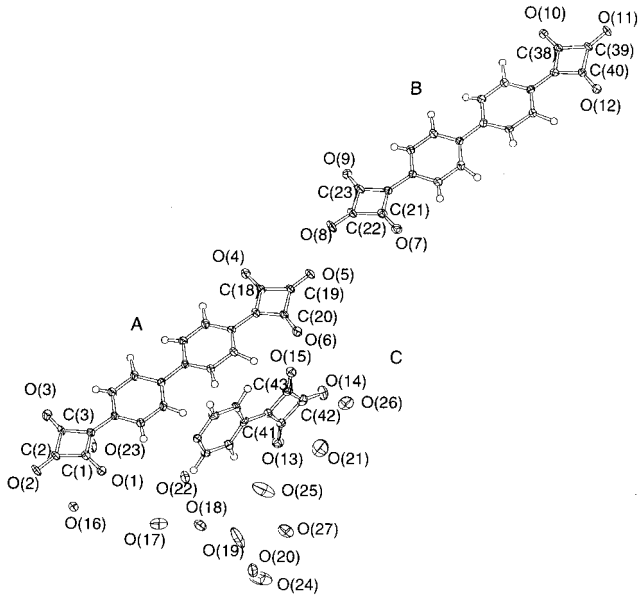

Figure 1. ORTEP drawing (probability 50%) of **BSQB**·4H_2O at 103 K. The **BSQB** molecules (A, B, and 0.5C) are shown together with O(16)−O(27) of the water molecules.

is expected to be sufficiently small. In fact, **BSQB** afforded a hydrated crystal, **BSQB**·4H_2O, when it was recrystallized from aqueous solution. In the crystal, there is a 1D hydrogen-bonded chain composed of **BSQB** and a cluster of water molecules. Here we report the proton dynamics along the 1D hydrogen-bonded chain in the **BSQB**·4H_2O crystal.

Results and Discussion

A. X-ray Crystallographic Analysis of BSQB·4H_2O. The crystal structure of **BSQB**·4H_2O was determined at 103 K (Figures 1 and 2; Table 1).[6] The asymmetric unit consists of two and a half molecules of **BSQB** (A, B, and 0.5C) and 10 water molecules. The accuracy of the location of the oxygen atoms of the water molecules was within one third of the estimated standard deviation (occupancies of oxygen atoms were 1.0 for O(16)−O(23) and 0.5 for O(24)−O(27)). The arrangement of **BSQB**(A) and **BSQB**(B) on the [1−1 1] plane is shown in Figure 2, **BSQB**(C) being omitted for clarity. The squaryl groups of **BSQB**(A) and **BSQB**(B) are connected by a cluster of four water molecules (w_i, $i = 1-8$) through hydrogen bonds along the vertical direction with respect to the long molecular axis of **BSQB**. These hydrogen bond distances are in the range 2.50−3.10 Å.

The **BSQB** molecules on the sheet are stacked along the [1 −1 1] direction, sliding slightly off along the long molecular axis due to the intermolecular electrostatic repulsion between negatively charged squaric acid moieties. Accordingly, the channel created between two parallel **BSQB** molecules is not strictly perpendicular to the stacking direction. **BSQB**(C) is incorporated in this channel, whose long molecular axis is inclined 30° toward the sheet composed of **BSQB**(A) and **BSQB**(B) (Figure 3). Thus, the hydrated crystal of **BSQB** can be regarded as a "self-trapped" host−guest-type crystal.

Since squaric acid derivatives are highly acidic, they are partially deprotonated in water: the pK_a of phenylsquaric acid in aqueous solution is −0.22,[7] which means the equilibrium ratio of the neutral species relative to the deprotonated species in solution is only about 0.6. Under this circumstance, it is expected that a squaric acid derivative affords an ionic hydrated salt. A close examination of the X-ray diffraction data revealed that **BSQB** exists mostly as a deprotonated form in the hydrated crystal. It should be noted that the C−O bond lengths between the enol group and the carbonyl group of **BSQB**(A) are different: The difference between C(1)−O(1) (C(18)−O(4)) and C(3)−O(3) (C(20)−O(6)) is ca. 0.08 Å (Table 2). The significant difference in the C−O bond lengths may be due to the environment around **BSQB**(A); the carbonyl and enol oxygen atoms at the 1- and 3-positions of the squaryl groups are hydrogen bonded with water molecules, e.g., O(1)−w_5, O(3)−w_2, O(4)−w_8, and O(6)−w_3. Very short intermolecular O−O distances (ca. 2.5 Å) between O(1) and the oxygen atom of w_5, and also between O(4) and w_8, exist. Such short O−O distances must be ascribed to an ionic hydrogen bond between the enolate group and the oxonium ion that is formed through protonation by the squaryl group, and a bond alternation in **BSQB**(A) results from localization of the negative charge at the enolate groups due to the contact ion-pair formation. In contrast, the C−O bond lengths of the two squaryl groups of **BSQB**(B) are almost the same (Table 2). This result suggests that the C−O bonds at the 1- and 3-positions of the squaryl group are equivalent and that negative charges are equally distributed on these squaryl groups. The situation may be caused by the symmetrical hydrating environment around **BSQB**(B). Consequently, we conclude that the 1D hydrogen-bonded chain consists of the anionic **BSQB** and protonated and neutral water molecules.

X-ray diffraction analysis was also carried out at 200 and 273 K. The temperature dependence of the unit cell dimensions and the cell volume are in the range for thermal expansion of the crystal (Table 1). In addition, the location of atoms in the unit cell does not change significantly with increasing temperature. When the average of the equivalent temperature factors of heavy atoms was plotted against the square root of temperature, the correlation in Figure 4 was obtained. The temperature dependence of the thermal parameters for the oxygen atoms of the water molecules (w_1−w_{12}) was much larger than those of the constituent atoms of **BSQB** molecules (A, B, and C). This means that the dynamic disorder and orientation of water molecules becomes pronounced at elevated temperatures, as also evidenced in the deuterium NMR spectrum (vide infra).

X-ray crystallographic analysis revealed two types of hydrated water. Eight water molecules out of 10 per 2.5 **BSQB** molecules (A, B, and 0.5 C) form a hydrogen-bonded chain that connects **BSQB** (A, B) molecules, whereas two water molecules are loosely bound to the guest **BSQB** molecule (C). These crystal water molecules became disordered at elevated temperature (vide ante). The dehydrating process of the crystal water was monitored by thermogravimetry. A gradual loss of two water molecules out of 10 was observed from room temperature to 300 K. The two water molecules were assigned to loosely bound water molecules at the top and bottom of the guest **BSQB**(C). A distinct two-step decrease in weight was observed above 300 K: Four water molecules per 2.5 **BSQB** molecules were lost at 330 K, and another set of four water molecules was lost at 365 K. An endothermic peak was also detected at each of these temperatures by differential scanning calorimetry (DSC). No exo- or endothermic peaks assignable to a phase transition were observed in the range 180−330 K.

B. Dynamics of Water Molecules and Oxonium Ions by Magic Angle Spinning Deuterium NMR. To elucidate the local mobility of water molecules and oxonium ions in the hydrated crystal of **BSQB**, the magic angle spinning deuterium

(6) Johnson, C. K. *ORTEP II, Report ORNL-5138*; Oak Ridge National Laboratory: Oak Ridge, TN, 1976.

(7) Patton, E.; West, R. *J. Am. Chem. Soc.* **1973**, *95*, 8703−8707.

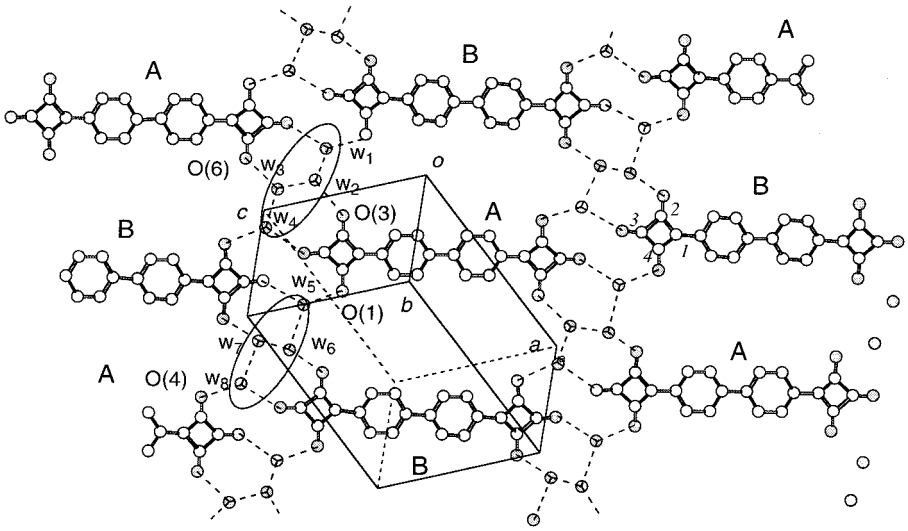

Figure 2. Crystal structure of **BSQB**·4H_2O at 103 K. Guest molecules are omitted. Broken lines represent hydrogen bonds. Clusters of four water molecules are circled.

Table 1. Crystallographic Data of **BSQB**·4H_2O Measured at 103, 200, and 273 K

formula	$C_{50}H_{45}O_{25}$		
formula weight	1045.89		
crystal color, habit	yellow, block		
space group	$P\bar{1}$		
T/K	103(1)	200(1)	273(1)
crystal system	triclinic	triclinic	triclinic
a/Å	14.095(3)	14.123(1)	14.202(2)
b/Å	15.649(4)	15.694(1)	15.805(3)
c/Å	11.585(2)	11.649(1)	11.653(2)
a/deg	109.30(1)	109.865(4)	110.15(1)
β/deg	97.92(1)	98.362(5)	98.138(10)
γ/deg	94.69(1)	94.384(5)	94.54(1)
V/Å^3	2366.3(1)	2380.2(1)	2407.6(1)
Z		2	
residuals: R, R_w	0.0988	0.0758	0.0764
residuals: R_1	0.0873	0.0864	0.0784
goodness-of-fit indicator	7.111	7.374	5.748

Table 2. C−O Bond Lengths and Differences at the 1- and 3-Positions of the Squaryl Groups of **BSQB** at 103 K

type of **BSQB** molecule	atom−atom	distance/Å	difference/Å
A	C(1)−O(1)	1.290(6)	
	C(2)−O(2)	1.216(4)	
	C(3)−O(3)	1.224(6)	0.076(6)
	C(18)−O(4)	1.298(6)	
	C(19)−O(5)	1.209(4)	
	C(20)−O(6)	1.214(6)	0.084(6)
B	C(21)−O(7)	1.260(6)	
	C(22)−O(8)	1.215(5)	
	C(23)−O(9)	1.253(6)	0.007(6)
	C(38)−O(10)	1.253(5)	
	C(39)−O(11)	1.204(4)	
	C(40)−O(12)	1.253(5)	0.000(5)
C	C(41)−O(13)	1.252(5)	
	C(42)−O(14)	1.225(5)	
	C(43)−O(15)	1.257(5)	0.005(5)

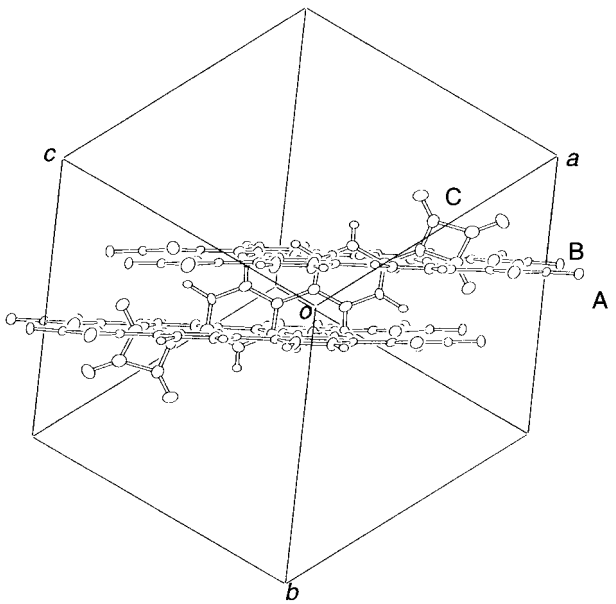

Figure 3. Crystal structure of **BSQB**·4H_2O viewed along the [111] direction. Water molecules are omitted for clarity.

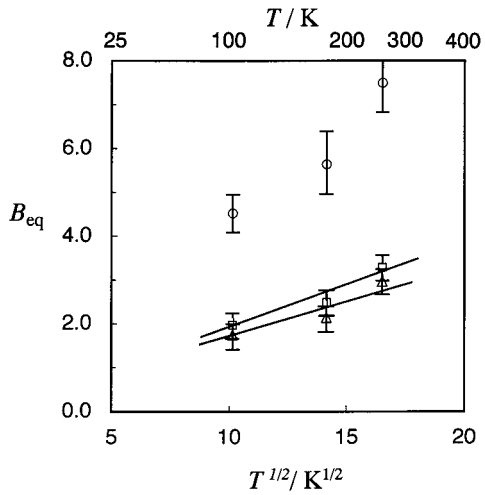

Figure 4. Temperature dependence of averaged equivalent temperature factors (B_{eq}). Averaged parameters of heavy atoms in **BSQB**(A, B), **BSQB**(C), and water molecules (w_1 − w_{12}) are represented by △, □, and o, respectively.

NMR spectrum of powdered **BSQB**·4D_2O crystals was measured. The temperature dependence of the spectral pattern in the range 186−310 K is shown in Figure 5. Peaks in the middle are resonance lines with isotropic shifts, whereas peaks at the sides (marked with asterisks) are spinning sidebands with a spinning speed of 9 kHz. The spectrum at 186 K clearly showed that the central signal was split into a doublet at 6.8 and 22 ppm: the higher field peak was assigned to hydrogen-bonded

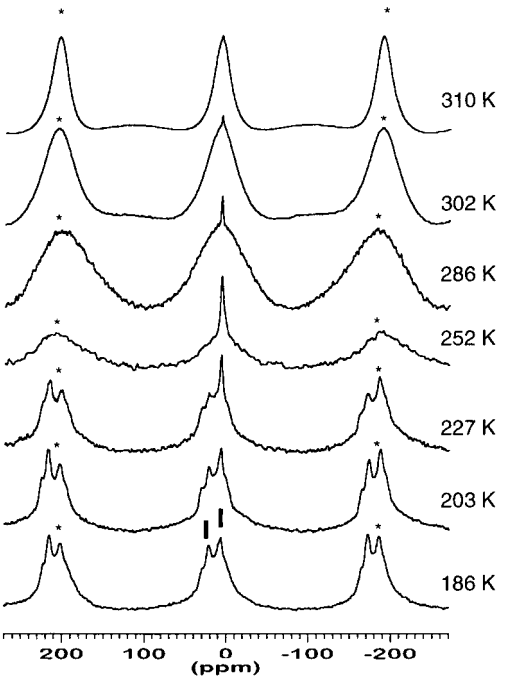

Figure 5. Magic angle spinning deuterium NMR spectrum of **BSQB**·$4D_2O$ (spinning speed, 9 kHz). The central signals are resonance lines with isotropic shifts; other peaks (marked with asterisks) are spinning sidebands. The peaks of water molecules and oxonium ions in the spectrum at 186 K are indicated by thick vertical bars.

water molecules with a normal hydrogen bond distance; the lower field peak corresponds to the hydrogen-bonded oxonium ions. At 252 K, the two peaks merged into a broad signal, which became narrower with increasing temperature. A sharp signal overlapping the broad signal comes from relatively free water molecules. This result clearly indicates that deuterons are exchanged between water molecules and oxonium ions around 250 K and that deuterons eventually migrate within the hydrogen-bonded cluster of water molecules that connect **BSQB**(A) and **BSQB**(B). At 252 K, the exchange rate of a deuteron exchanging between a water molecule and an oxonium ion is comparable to the difference in the resonance frequencies between the peaks at 6.8 and 22 ppm (ca. 700 Hz).

C. Temperature and Frequency Dependence of Dielectric Response. Ac dielectric measurements on the hydrated crystal of **BSQB** were carried out with an LCR meter. The surface on which the gold leaf electrodes were attached was approximately perpendicular to the *a* axis.[8] Accordingly, the applied electric field has a significant component parallel to the *a* axis. The temperature dependence of the dielectric permittivity (ϵ') at 1, 10, and 100 kHz is shown in Figure 6. The ϵ' value remained constant at ca. 7 from cryogenic temperatures to around 250 K. Above 250 K, ϵ' started to increase dramatically and reached 4.7×10^4 at 340 K and 1 kHz. This frequency dependence of ϵ' above 250 K corresponds well with the exchange rate of ca. 700 Hz at 252 K determined by magic angle spinning deuterium NMR. Whereas the temperature dependence of the permittivity was reversible below 300 K, it decreased irreversibly above 300 K due to the loss of crystal water molecules (vide ante).

The frequency dependencies of ϵ' and ϵ'' were measured at 280 K over the frequency range of 10^6-20 Hz. Reflecting the fact that the increase of both ϵ' and ϵ'' is monotonic as the ac

(8) As seen from Figure 3, the direction of the molecular stacking or the hydrogen-bonded chain is not exactly parallel to a crystal axis. Furthermore, the crystal has a brick-like shape. Consequently, it was difficult to identify the crystal surface on which the gold leaves were attached.

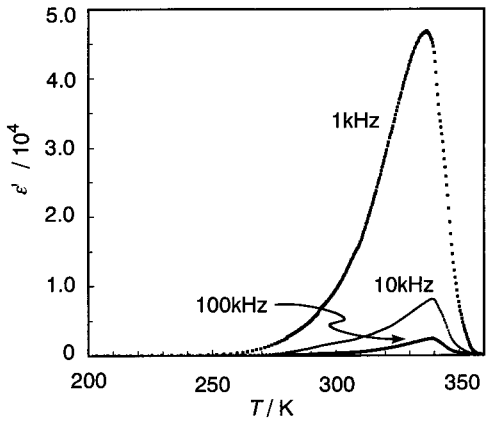

Figure 6. Temperature dependence of the permittivity (ϵ') of a single crystal of **BSQB**·$4H_2O$ along the *a* axis. The frequency dependencies at 1, 10, and 100 kHz are also plotted.

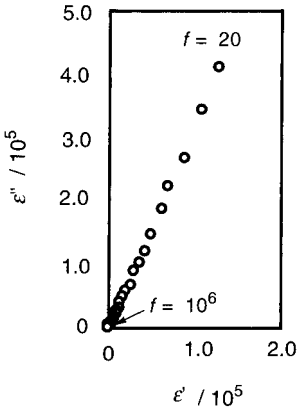

Figure 7. Cole−Cole plot of a single crystal of **BSQB**·$4H_2O$ along the *a* axis at 280 K.

frequency decreased, a Cole−Cole plot gave a straight line instead of the typical half-circle trace (Figure 7). In such a case, a dc conductivity contribution may be suspected because an ac current of extremely low frequency can be regarded as a dc current (vide infra), although the permittivity of the crystal was not affected by changes in the external electric field in the range 5.0−200 V cm^{-1}.

The dielectric response of the hydrated crystal of **BSQB** is in contrast with previously reported results for inorganic hydrated crystals with a 2D or 3D hydrogen-bonded network.[9] X-ray crystallographic analysis of Na_2HPO_4·$12H_2O$, for example, proved the 3D hydrogen-bonded structure of hydrating water molecules.[10] Analysis of the dielectric dispersion in a single crystal of Na_2HPO_4·$12H_2O$ gave a half-circular Cole−Cole plot, which indicates dielectric behavior caused by a Debye-type mechanism.[11] In contrast, orientational defects in the 2D hydrogen-bonded water molecules in $Cd(H_2O)_2Ni(CN)_4$·$4H_2O$ are generated much more easily than in the case of hexagonal ice.[12] The reason for this is that protons located above or below the hydrogen-bonded plane cannot participate in the 2D hydrogen-bonded network. The dynamic response of water molecules in these systems is believed to be derived from orientational defects as proposed by Bjerrum.[13]

(9) (a) Kiriyama, R.; Ibamoto, H. *Bull. Chem. Soc. Jpn.* **1953**, *26*, 109. (b) Kiriyama, R.; Ibamoto, H. *Bull. Chem. Soc. Jpn.* **1954**, *27*, 32−35. (c) Kiriyama, R.; Ibamoto, H. *Bull. Chem. Soc. Jpn.* **1954**, *27*, 323−326.

(10) Ruben, H. W.; Templeton, D. H.; Rosenstein, R. D.; Olovsson, I. *J. Am. Chem. Soc.* **1961**, *83*, 820−824.

(11) Kiriyama, R.; Saito, Y. *Bull. Chem. Soc. Jpn.* **1953**, *26*, 531.

(12) Okishiro, K.; Yamamuro, O.; Tsukushi, I.; Matsuo, T.; Nishikiori, S.; Iwamoto, T. *J. Phys. Chem. B* **1997**, *101*, 5804−5809.

In contrast, the dielectric response of the **BSQB**·$4H_2O$ crystal originated from the dynamics in the 1D hydrogen-bonded chain. The dielectric response of **BSQB**·$4H_2O$ cannot be interpreted in terms of Bjerrum's mechanism, in which the existence of a hydrogen-bonded network is postulated. A comparable model may be searched for in 1D molecular dielectrics such as TTF-chloranil, TTF-bromanil, or $TTeC_1TTF$-TCNQ complex.[14] The characteristic dielectric response of these compounds is derived from the migration of boundaries of domains composed of ferroelectrically ordered ionic species. Since the dynamic behavior of proton transfer along the 1D-chain resemble that of charged soliton in ionic dielectrics,[1c,d] the mechanism of the polarity inversion in this hydrated crystal may be expressed as a solitonic motion of the domain boundaries.

D. Solitonic Motion of Charged Domain Boundaries in 1D Hydrogen-Bonded Chain. Taking into account the above examples, it is reasonable to assume that the mechanism of the dielectric behavior of the hydrated crystal of **BSQB**·$4H_2O$ is similar to that of the aforementioned 1D molecular dielectrics. In the 1D hydrogen-bonded chain, an enolate group of the squaryl moiety and an oxonium ion form an ion pair with an ionic dipole. Since the squarate ion has C_{2v} symmetry intrinsically, it can form an ion pair with an oxonium ion on the other side of the squaryl group as well. Therefore it is not likely that such a fluctuating 1D chain constitutes a *single* ferroelectric domain structure. The 1D hybrid hydrogen-bonded chain must be constructed by ferroelectrically aligned domains, each of which is composed of parallel ionic dipoles (Figure 8). As shown in Figure 8, the domain boundary of this 1D hydrogen-bonded chain consists of a squarate ion sandwiched by two oxonium ions (positively charged domain boundary), or a squarate ion with two neutral water molecules (negatively charged domain boundary). These domain boundaries can move when a proton migrates from the oxonium ion to the adjacent water molecule (Figure 9, top line). Then the squarate ion in the middle will be sandwiched by two oxonium ions to become a new domain boundary (Figure 9, second line). In other words, a proton relay from a protonated water cluster to an adjacent water cluster is mediated in terms of localization and delocalization of negative charge in the squarate ion.

To obtain information on the dynamics of the charged domain boundaries, the frequency dependence of the loss angle of tan δ ($= \epsilon''/\epsilon'$), was measured in the range 290−200 K. The results are plotted in Figure 10. Although the tan δ values were scattered over a wide frequency range, there was a distinct maximum at 3.0 kHz in the frequency dependence plot at 290 K. This maximum shifted to the lower frequency side with decreasing temperature. Another maximum around 100 kHz was observed at 250 K and was also shifted to the lower frequency side as the temperature decreased. The relaxation time is considerably slower than the time scale for the proton transfer of the tautometric molecule in the gas phase[15] or the zero-dimensional hydrogen-bonded system in the solid state.[16] Such a *pronounced and slow* response can only be rationalized by the movement of the charged domain boundaries coupled with correlated proton transfer.

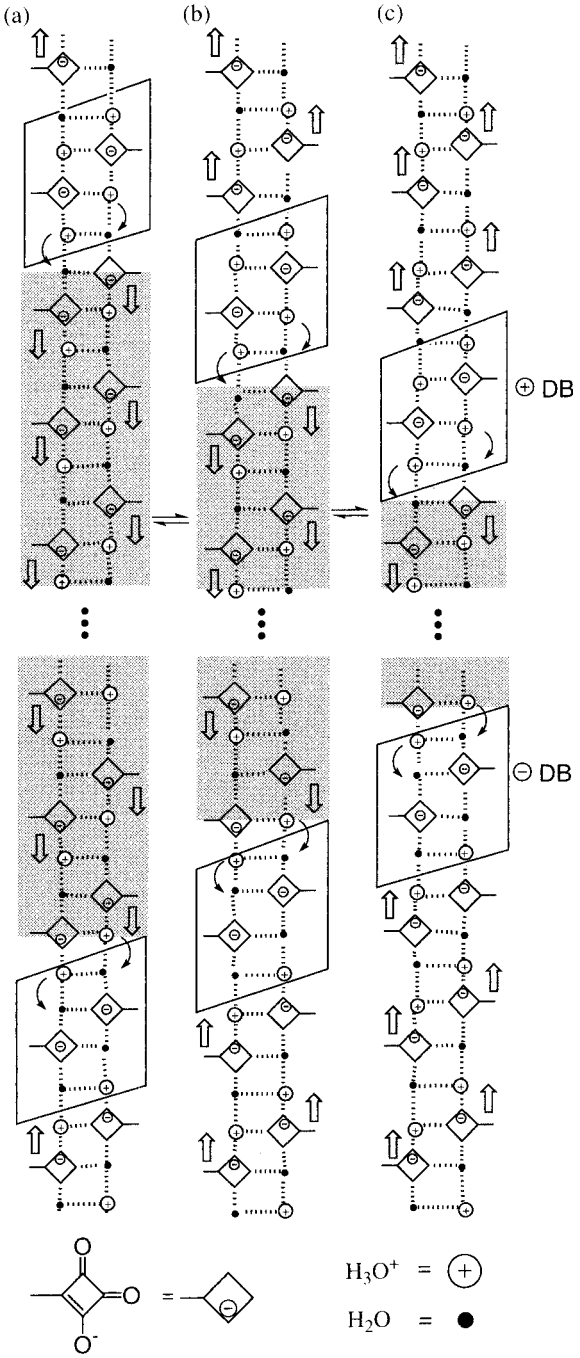

Figure 8. Schematic drawing of the collective polarity inversion and the migration of the domain boundary derived from sequential proton relay. Curved arrows represent the migration of protons. Thick arrows denote the direction of the dipole moment. ⊕DB and ⊖DB represent the positive and negative domain boundaries, respectively.

Since the almost straight line in the Cole−Cole plot reflects the contribution of the dc conductivity (Figure 7), the charged

(13) Bjerrum, N. *Science* **1952**, *115*, 385−390.

(14) (a) Tokura, Y.; Koshihara, S.; Iwasa, Y.; Okamoto, H.; Komatsu, T.; Koda, T.; Iwasawa, N.; Saito, G. *Phys. Rev. Lett.* **1989**, *63*, 2405−2408. (b) Okamoto, H.; Mitani, T.; Tokura, Y.; Koshihara, S.; Komatsu, T.; Iwasa, Y.; Koda, T.; Saito, G. *Phys. Rev.* **1991**, *B43*, 8224−8232. (c) Okamoto, H.; Tokura, Y.; Koda, T. *Phys. Rev.* **1987**, *B36*, 3858−3867.

(15) (a) Baughcum, S. L.; Duert, G. N.; Rowe, W. F.; Smith, Z.; Wilson, E. B. *J. Am. Chem. Soc.* **1981**, *103*, 6296−6303. (b) Baughcum, S. L.; Smith, Z.; Wilson, E. B.; Duert, G. N. *J. Am. Chem. Soc.* **1984**, *106*, 2260−2265. (c) Bondybey, V. E.; Haddon, R. C.; English, J. H. *J. Chem. Phys.* **1984**, *80*, 5432−5437. (d) Turner, P.; Baughcum, S. L.; Coy, S. L.; Smith, Z. *J. Am. Chem. Soc.* **1984**, *106*, 2265−2267. (e) Barbara, P. F.; Walsh, P. K.; Brus, L. E. *J. Phys. Chem.* **1989**, *93*, 29−34. (f) Nishi, K.; Sekiya, H.; Mochida, T.; Sugawara, T.; Nishimura, Y. *J. Chem. Phys.* **2000**, *112*, 5002−5011. (g) Nishi, K.; Sekiya, H.; Hamabe, H.; Nishimura, Y.; Mochida, T.; Sugawara, T. *Chem. Phys. Lett.* **1996**, *257*, 499−506.

(16) (a) Geshi, K *J. Phys. Soc. Jpn.* **1980**, *48*, 886. (b) Mochida, T.; Izuoka, A.; Sugawara, T.; Moritomo, Y.; Tokura, Y. *J. Chem. Phys.* **1994**, *101*, 7971−7974. (c) Noda, Y.; Tamura, I.; Kuroiwa, Y.; Mochida, T.; Sugawara, T. *J. Phys. Soc. Jpn.* **1994**, *63*, 4286−4289. (d) Tamura, I.; Noda, Y.; Kuroiwa, Y.; Mochida, T.; Sugawara, T. *J. Phys.: Condens. Matter* **2000**, *12*, 8345−8356.

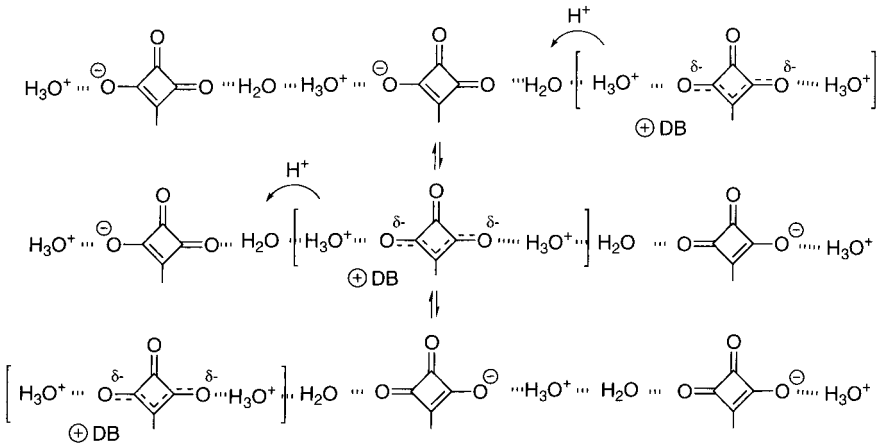

Figure 9. Movement of a positive domain boundary in a 1D hybrid hydrogen-bonded chain.

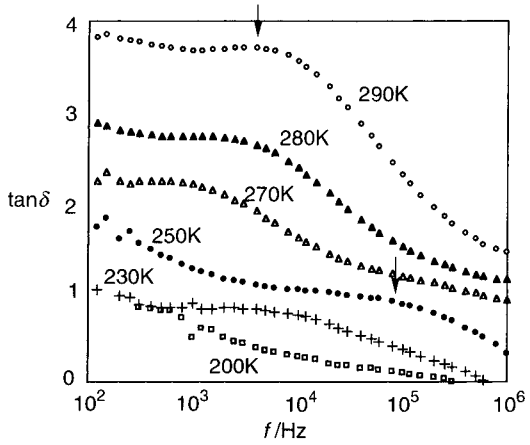

Figure 10. Frequency dependence of the loss tangent (tan $\delta = \epsilon''/\epsilon'$) at 200 K (□), 230 K (+), 250 K (●), 270 K (△), 280 K (▲), and 290 K (○).

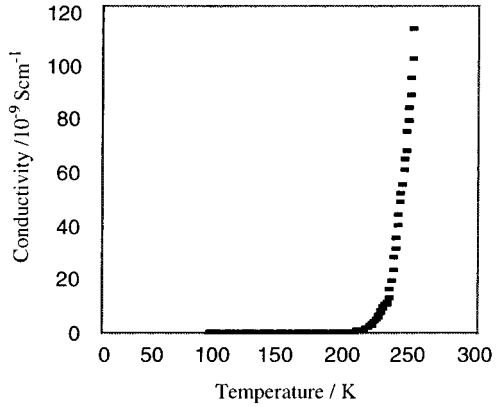

Figure 11. Temperature dependence of the dc conductivity of a single crystal of **BSQB**·$4H_2O$ along the *a* axis.

domain boundary can be designated as a charged soliton along the 1D hydrogen-bonded chain. When the dc conductivity of a single crystal of **BSQB**·$4H_2O$ was measured along the *a* axis, the conductivity started to increase at temperatures higher than 150 K, reaching 0.11 μS cm^{-1} at 240 K at an electric field of ca. 10^3 V cm^{-1} (Figure 11). It should be noted that the temperature dependence of the conductivity corresponds to the rise observed in the temperature dependence of the permittivity (Figure 6). Thus the observed direct current is best interpreted as the solitonic migration of the charged domain boundaries, which can move to an electrode under an external electric field, oscillating with an inherent frequency of ca. 3 kHz at 290 K. The possibility that the dc conductivity is derived from electronic transport along the π-stack of **BSQB** can be excluded, because **BSQB** is neither an electron donor nor an electron acceptor and no charge-transfer absorptions or interband transitions are detected in the UV or near-IR spectrum of the crystal of **BSQB**·$4H_2O$. Accordingly, the detection of the dc conductivity is not inconsistent with the solitonic motion of the charged domain boundaries along the 1D hydrogen-bonded chain.

Conclusion

An artificial 1D hydrogen-bonded chain composed of a cluster of partially protonated water molecules and highly polarizable π-conjugated dianions was constructed. This hybrid hydrogen-bonded chain exhibits an enhanced dielectric response with slow relaxation processes. An influence of the direct current was suggested by the frequency dependence of the dielectric response and the dc conductivity measurements. These dynamic features were well rationalized by the solitonic movement of domain boundaries created by charge defects along the hydrogen-bonded chain.

It is significant that the sequential proton relay was realized by using a hybrid chain composed of a cluster of water molecules and a π-conjugated dianion instead of an infinite hydrogen-bonded chain of water molecules. The hybrid structure creates a "soft environment" of a cluster of water molecules and oxonium ions, and a collective motion can be generated without a large formation (activation) energy. The system resembles a biological proton relay system composed of amino acid residues and clusters of water molecules. Proton transfer along this artificial system provides important insight into the mechanism of the active proton transport that membrane proteins exhibit.

Experimental Section

Preparation 4,4′-Bis(4-(1-methylethoxy)-2,3-dioxocyclobut-3-en-1-yl)biphenyl (1). 4,4′-Diiodobiphenyl (0.95 g, 2.22 mmol) and 4-(1-methylethoxy)-3-(tri-*n*-butylstannyl)cyclobut-3-ene-1,2-dione[17] (6.0 g, 4.44 mmol) were dissolved in 15 mL of distilled toluene. A solid mixture of dichlorobis(triphenylphosphine)palladium(II) (196 mg, 6 mol %) and copper iodide (52 mg, 6 mol %) was added to the solution, and the reaction mixture was stirred under N_2 at 50 °C for 12 h. The yellowish red precipitate was filtered, and the solvent was evaporated. The residue was dissolved in 25 mL of chloroform, the mixture was filtered, and the crude product was recrystallized from tetrahydrofuran (THF) to give 0.45 g (1.26 mmol, 57%) of yellow solid: ^{1}H NMR (270 MHz, $CDCl_3$; ppm) δ 8.16 (d, J = 8.42 Hz, 4H), 7.79 (d, J =

(17) Liebeskind, L. S.; Yu, M. S.; Wang, J.; Hagen, K. S. *J. Am. Chem. Soc.* **1993**, *115*, 9048−9055.

8.42 Hz, 4H), 5.66 (hept, $J = 6.23$ Hz, 2H), 1.59 (d, $J = 6.23$ Hz, 12H); ^{13}C NMR (68 MHz, $CDCl_3$; ppm) δ 194.36, 192.72, 192.26, 173.05, 143.58, 128.25, 127.75, 127.62, 80.40, 23.06; IR (KBr; cm^{-1}) 2979, 2956, 1521, 1498, 1468 (ν_{CH3}), 1779, 1746 ($\nu_{C=O}$), 1684, 1607, 1588 ($\nu_{C=C}$), 1397 (ν_{CO}), 1101, 1086 ($\nu_{CH(CH3)2}$), 831, 802, 776 (δ_{CH}).

4,4′-Bis(4-hydroxy-2,3-dioxocyclobut-3-en-1-yl)biphenyl (BSQB). The minimum amount of THF was used to dissolve 0.45 g of **1** (1.26 mmol), and the resulting solution was treated with concentrated hydrochloric acid (10 mL). The reaction mixture was allowed to stir at room temperature for 6 h. Distilled water (300 mL) was added to this mixture, and the solution was then evaporated. Recrystallization from THF gave yellow block-shaped crystals of 4,4′-bis(4-hydroxy-2,3-dioxocyclobut-3-en-1-yl)biphenyl (**BSQB**) (0.40 g, 91%): ^{1}H NMR (270 MHz, DMSO-d_6; ppm) δ 8.26 (d, $J = 6.96$ Hz, 4H), 7.85 (d, $J = 6.96$ Hz, 4H); ^{13}C NMR (68 MHz, DMSO-d_6; ppm) δ 210.64, 196.66, 173.65, 139.71, 130.56, 126.76, 124.81; IR (KBr; cm^{-1}) 2500 ($\nu_{OHO=C}$), 1795, 1784, 1773, 1729 ($\nu_{C=O}$), 1606, 1553, 1526 (ν_{CH}), 1422, 1413, 1399, 1392 (ν_{CO}), 839, 805, 639 (δ_{CH}). Single crystals of hydrated **BSQB** were obtained by slow evaporation of the solvent from a 5% aqueous solution of THF. Yellow block-shaped crystals were obtained (the largest size was ca. $2.0 \times 0.8 \times 1.0$ mm^3).

X-ray Crystallography. A single crystal of **BSQB** was sealed into a glass fiber with an aliquot of water and then mounted. Measurements were made at $T = 103$, 200, and 273 K on a Rigaku R-AXIS-IV imaging plate area detector with graphite-monochromatized Mo Kα radiation ($\lambda = 0.710\,73$ Å). The number of water molecules was determined by density measurement using the flotation method. Indexing was performed from three oscillations that were exposed for 5.0 min. The crystal-to-detector distance was 105.0 mm, with the detector at zero swing position. Readout was performed in the 0.1 mm pixel mode. The data were collected to a maximum 2θ value of 55°. A total of 35 3.00° oscillation images were collected, each being exposed for 60.0 min. Calculations were carried out on an SGI Indy using the teXsan[18] crystallographic software package from Molecular Structure Corp. The structure was solved by direct methods using SIR92[19] and expanded by Fourier techniques. The non-hydrogen atoms were refined anisotropically. The refinement of the structure was performed by a full-matrix least-squares method.[20] $C_{50}H_{45}O_{25}$: FW 1045.89, triclinic, $P\bar{1}$, $Z = 2$. Other crystallographic data at each temperature are shown in Table 1.

Dielectric Measurement. Dielectric permittivity was measured with an alternating electric field in the range 5.0−200 V cm^{-1} and recorded with a Hewlett-Packard 4274A LCR meter in the frequency range of 20 Hz to 1 MHz. The temperature of the sample was measured by an Au/Fe chromel thermocouple. Gold leaves were attached on both planes of the crystal.

Dc Conductivity. A 40 μm thick crystal was sandwiched between two gold-plate electrodes, and its temperature was monitored with a copper−constantan thermocouple. A 100 V, 0.1 Hz triangular wave was applied to the crystal, and its conductivity was evaluated from the slope of the longer side of the parallelogram in the $I-V$ plot.

Thermal Analysis. Thermogravimetry was carried out with a Seiko TG/DTA 5200 instrument in the temperature range 293−573 K with a heating rate of 3 K min^{-1}. Differential scanning calorimetry was performed with a TA Instruments differential scanning calorimeter in the temperature range 180−400 K with the same heating and cooling rates.

Deuterium NMR. The magic angle spinning deuterium NMR spectrum was measured with a Bruker DSX 300 spectrometer at the resonance frequency of 45 MHz in the temperature range 186−310 K. A 4 mm zirconia rotor and spinning rate of 9 kHz were used. The thermometer of the magic angle spinning NMR probe was carefully calibrated.[21] The deuterated sample was prepared by recrystallization of **BSQB** from a mixture of THF and heavy water. **BSQB**·4D_2O was coarsely powdered and sealed into the zirconia rotor.

Acknowledgment. This work was supported by a Grant-in-Aid for Scientific Research on Priority Areas (A) (No. 10146103) from the Ministry of Education, Science, Sports and Culture, Japan.

Supporting Information Available: Experimental details; coordinates, thermal parameters, bond lengths, and angles (PDF). This material is available free of charge via the Internet at http://pubs.acs.org.

JA010519A

(18) *Single-Crystal Structure Analysis Software, Version 1.6*; Molecular Structure Corp.: The Woodlands, TX, 1993.

(19) Burla, M. C.; Camalli, M.; Cascarano, G.; Giacovazzo, C.; Polidori, G.; Spagna, R.; Viterbo, D. *J. Appl. Crystallogr.* **1989**, *22*, 389−393.

(20) Busing, W. R.; Martin, K. O.; Levy, H. A. ORFLS. *A FORTRAN Crystallographic Least Squares Program. Report ORNL-TM-305*; Oak Ridge National Laboratory: Oak Ridge, TN, 1962.

(21) Maruta, G.; Takeda, S.; Imachi, R.; Ishida, T.; Nogami, T.; Yamaguchi, K. *J. Am. Chem. Soc.* **1999**, *121*, 424−431.